Supporting Information

# Organic Solar Cells Based On $Cu_2O$/FBT-TH4 Anode Buffer Layer with Enhanced Power Conversion Efficiency and Ambient Stability

*Yaxiong Guo[a], Hongwei Lei[a], Liangbin Xiong[a,b], Borui Li[a], Guojia Fang[a*]*

[a] Key Lab of Artificial Micro- and Nano-Structures of Ministry of Education of China, School of Physics and Technology, Wuhan University, Wuhan 430072, P. R. China. *E-mail: gjfang@whu.edu.cn

[b] School of Physics and Electronic-information Engineering, Hubei Engineering University, Xiaogan, 432000, P. R. China.

## 1. Experimental details

### 1.1. Sample preparations and characterizations

The donor polymer PffBT4T-2OD were purchased from 1-material Chemscitech, and used as received. The acceptor $PC_{71}BM$ are purchased from nano-c Company and used as received. PEDOT:PSS (Baytron Al 4083) was purchased from H. C. Starck GmbH, Germany. FBT-TH4 surfactant was provided by 1-material.

### 1.2. Device fabrication

The polymer solar cell device structure was ITO/HTMs/PffBT2T-2OD:$PC_{71}BM$/PDINO/Al. ITO–glass (15 Ω $sq^{-1}$) was precleaned by ultrasonication sequentially in a detergent, deionized water, acetone, and isopropyl alcohol. After drying, the ITO–glass was treated with UV-$O_3$ for 15 min. A solution-processed FBT-TH4 layer (5 mg/ml) was fabricated on the ITO/$Cu_2O$ film based on the sputtered method described in our previous report. Then, the BHJ layer was fabricated on the $Cu_2O$/FBT-TH4-modified anode in a glovebox by spin-coating (3000 rpm) a blend of PffBT4T-2OD:$PC_{71}BM$. The PffBT4T-2OD was blended with $PC_{71}BM$ at a weight ratio of 1:1.2 and dissolved in o-dichlorobenzene/chlorobenzene (CB)/1,8-diiodoctane (50%:50%:3% by volume), with a total concentration of 19.8 mg $mL^{-1}$, and the solution was stirred overnight at least 85°C. The active layer was spin-coated at 1000 rpm for 40 s (~250 nm). PDINO (1 mg $mL^{-1}$) solution was then spin-coated on the photoactive

layers at 3000 rpm for 30 s. Finally, Al (~100 nm) was evaporated through a shadow mask to define the active area of the devices (~0.04 $cm^2$) in a vacuum chamber ($1.0\times10^{-4}$ pa).

**1.3. Device characterization and measurement.**

The crystal structure of the $Cu_2O$ films were characterized by X-ray diffraction (XRD). Conventional XRD in Bragg-Brentano configuration has been performed by the same Bruker D8 Advance diffraction meter using Cu Kα radiation at 40 kV and 40 mA. Line traces were collected over 2θ values ranging from 20° to 80°. The transmittance of the films was measured by a UV-VIS-NIR spectrophotometer (CARY5000, Varian) in the 300-800 nm wavelength range at RT. The surface morphologies were made in a scanning electron microscope (SEM, FEI XL-30). X-ray photoelectron spectroscopy (XPS) and ultraviolet photoelectron spectroscopy (UPS) were performed using a XPS/UPS system (Thermo Scientific, ESCLAB 250Xi, USA). The compositions and chemical states of $Cu_2O$ film were examined by XPS. Before been tested, samples were sputtering-cleaned by the lower energy of Ar+ to remove atmospheric contamination in the XPS chamber for approximately 30 s, and the Ar+ gun was operated at 0.5 kV at a pressure of $1\times10^{-7}$ Pa. The vacuum pressure of the analysis chamber was better than $1\times10^{-8}$ Pa. The whole survey scan to identify the overall surface composition and chemical states were performed, using a monochromated Al Ka X-ray source (=1486.68

eV), detecting photoelectrons at a 150 eV pass energy and a channel width of 500 meV. The surface carbon signal at 284.6 eV was used as an internal standard. The work function and band energy position were calculated by UPS. UPS was carried out using Helium I$\alpha$ radiation from a discharge lamp operated at 90 W, a pass energy of 10 eV, and a channel width of 25 meV. A −9 V bias was applied to the samples, in order to separate the sample and analyze low-kinetic-energy cutoffs. The morphologies of different HTMs spin-casted on ITO were characterized by atomic force microscopy (AFM, SPM-9500J3, Shimadzu, Japan). The photoluminescence (PL) measurements were carried out under a 488 nm laser at RT and the emissions were collected via a HORIBA Jobin-Yvon monochromator. The current-voltage (*J-V*) curves of the devices were obtained using a computer-controlled Keithley 2400 Source Measure Unit and the device test was carried out under illumination of AM 1.5G, 100 mW $cm^{-2}$ (the light intensity was calibrated using a Si photodiode) at RT using a solar simulator. The corresponding incident photon-to-electron conversion efficiency (IPCE) spectrum was measured with a QE/IPCE measurement system (Enli Technology Co. Ltd).

**1.3. Measurements of the hole and electron mobility by the space-charge limited current (SCLC) method**

The hole and electron mobility was extracted by fitting the current density-voltage curves using the equation $J = 9\varepsilon\varepsilon_0\mu V^2/(8L^3)$,1 where ε is

the dielectric constant of the polymer (3), $\varepsilon_0$ is the permittivity of the vacuum ($8.85419\times10^{-12}$ C $V^{-1}$ $m^{-1}$), $\mu$ is the zero-field mobility, $J$ is the current density, $L$ is the thickness of the films, and $V = V_{appl}–V_{bi}$; herein $V_{appl}$ is the applied potential, and $V_{bi}$ the built-in potential which results from the difference in the work function of the anode and the cathode.

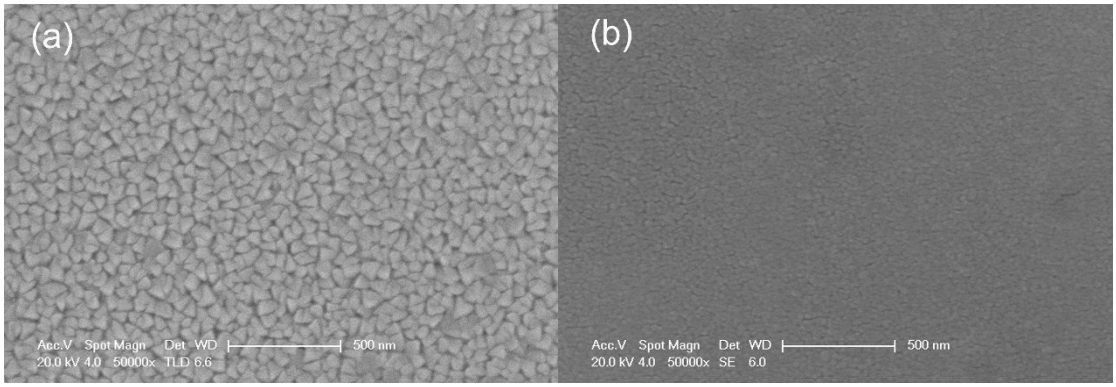


**Figure S1.** (a) SEM image of $Cu_2O$ film deposited on ITO substrate. (b) SEM image of FBT-TH4 film spin-casted on ITO/$Cu_2O$.

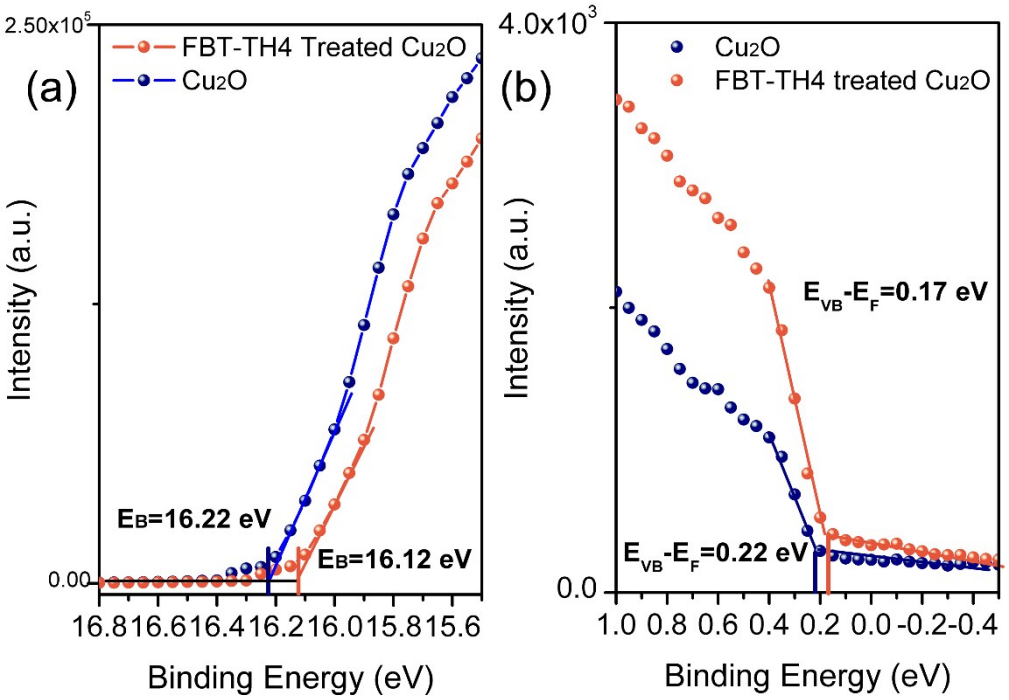


**Figure S2.** The work function (WF) and valence band maximum (VBM) and of $Cu_2O$ and FBT-TH4 treated $Cu_2O$.

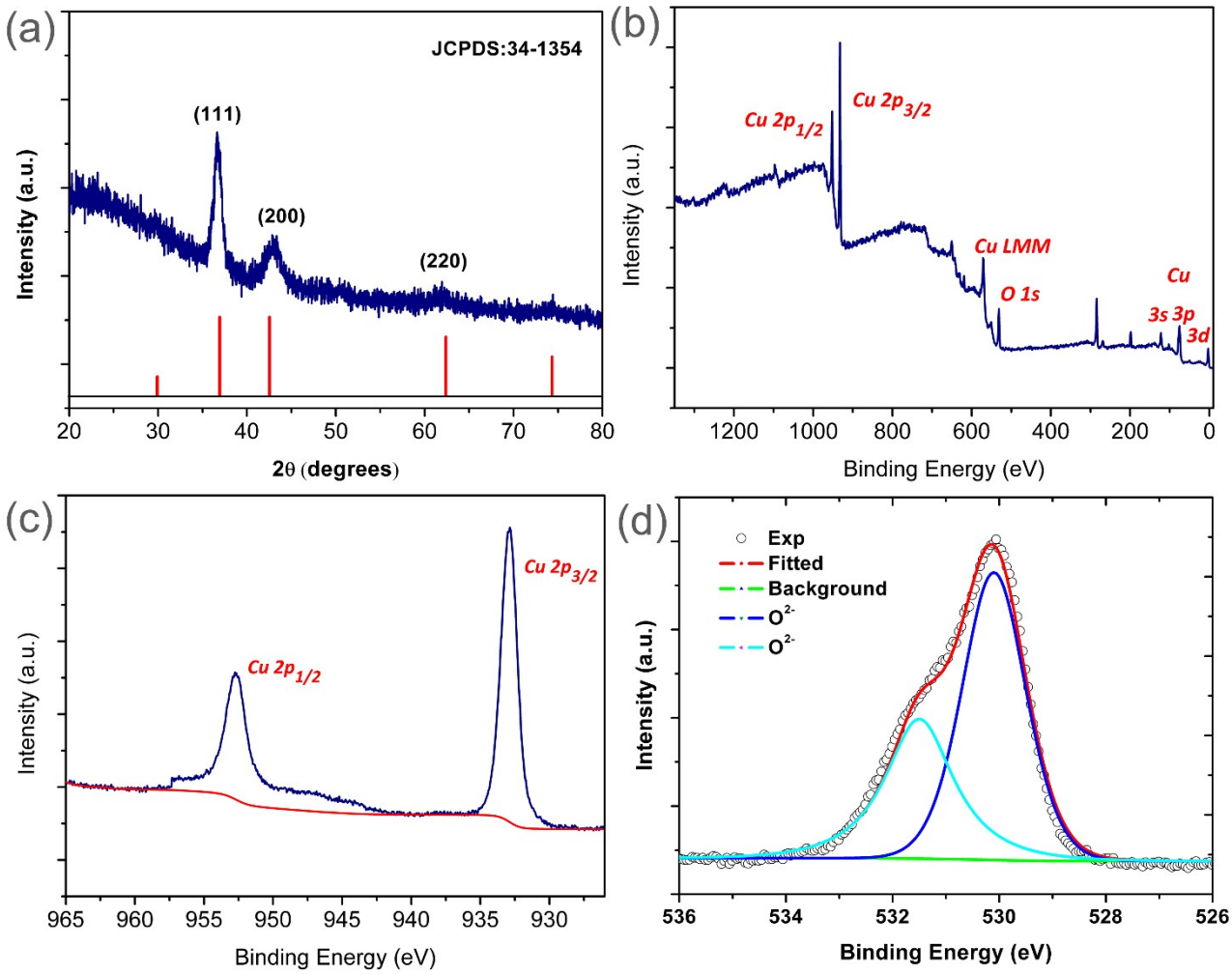


**Figure S3.** (a) Typical XRD pattern of $Cu_2O$ films in our study. XPS spectra of $Cu_2O$ film: (b) a whole survey of the XPS, (c) Cu 2p scan and (d) O 1s scan.

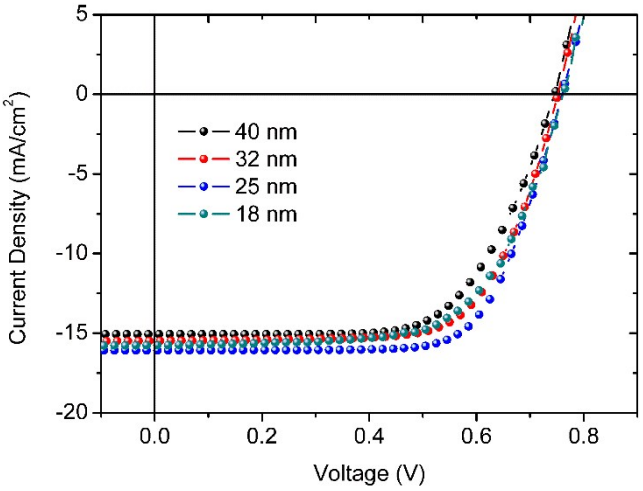


**Figure S4**. Device performance of the PSCs with $Cu_2O$ films of different thicknesses.

**Table S1.** Photovoltaic parameters of the PffBT4T-2OD:$PC_{71}BM$ based solar cell with untreated $Cu_2O$ layer as the HTM.

| *$Cu_2O$ thickness* [nm] | *Voc* [V] | *Jsc* [mA $cm^{-2}$] | *FF* [%] | *PCE* [%] |
|---|---|---|---|---|
| 40 | 0.76 | 15.06 | 66.1 | 7.57 |
| 32 | 0.76 | 15.47 | 68.1 | 8.01 |
| 25 | 0.76 | 16.07 | 69.4 | 8.46 |
| 18 | 0.77 | 15.73 | 64.5 | 7.81 |

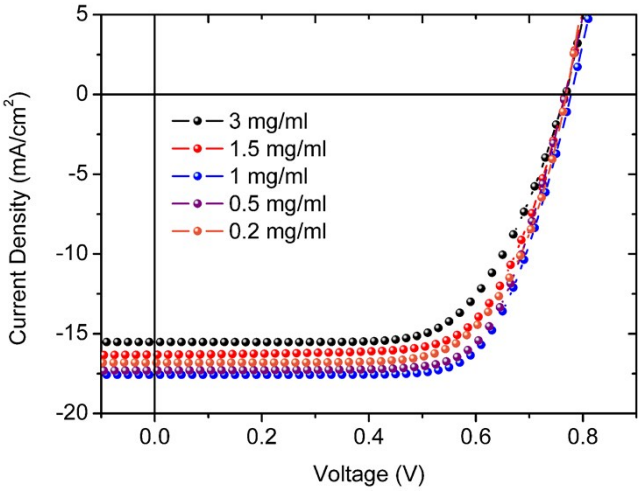


**Figure S5**. Device performance of the PSCs with FBT-TH4 of different concentrations. (Based on device architecture of ITO/$Cu_2O$/FBT-TH4/PffBT4T-2OD:$PC_{71}BM$/PDINO/Al)

**Table S2**. Device performance of the PSCs with FBT-TH4 of different concentrations.

| *FBT-TH4 concentration* [mg/ml] | *Voc* [V] | *Jsc* [mA $cm^{-2}$] | *FF* [%] | *PCE* [%] |
|---|---|---|---|---|
| 3 | 0.765 | 15.5 | 66.3 | 7.86 |
| 1.5 | 0.77 | 16.4 | 67.1 | 8.47 |
| 1 | 0.775 | 17.5 | 70.7 | 9.58 |
| 0.5 | 0.772 | 17.3 | 70.6 | 9.43 |
| 0.2 | 0.769 | 16.9 | 68.3 | 8.87 |

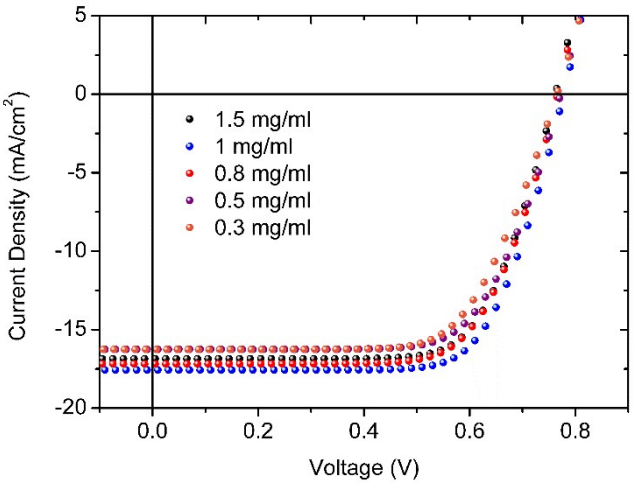


**Figure S6**. Device performance of the PSCs with PDINO layer of different concentrations. (Based on device architecture of ITO/$Cu_2O$/FBT-TH4/PffBT4T-2OD:$PC_{71}BM$/PDINO/Al)

**Table S3.** The effects of the concentration of the PDINO layer on the PffBT4T-2OD:$PC_{71}BM$ solar cell performance with the FBT-TH4 treated $Cu_2O$ layer as the HTMs.

| *PDINO concentration* [mg/ml] | *Voc* [V] | *Jsc* [mA $cm^{-2}$] | *FF* [%] | *PCE* [%] |
|---|---|---|---|---|
| 1.5 | 0.76 | 17.1 | 71.0 | 9.23 |
| 1 | 0.77 | 17.5 | 70.7 | 9.58 |
| 0.8 | 0.77 | 17.2 | 69.1 | 9.15 |
| 0.5 | 0.77 | 16.4 | 69.0 | 8.71 |
| 0.3 | 0.77 | 16.3 | 67.8 | 8.51 |

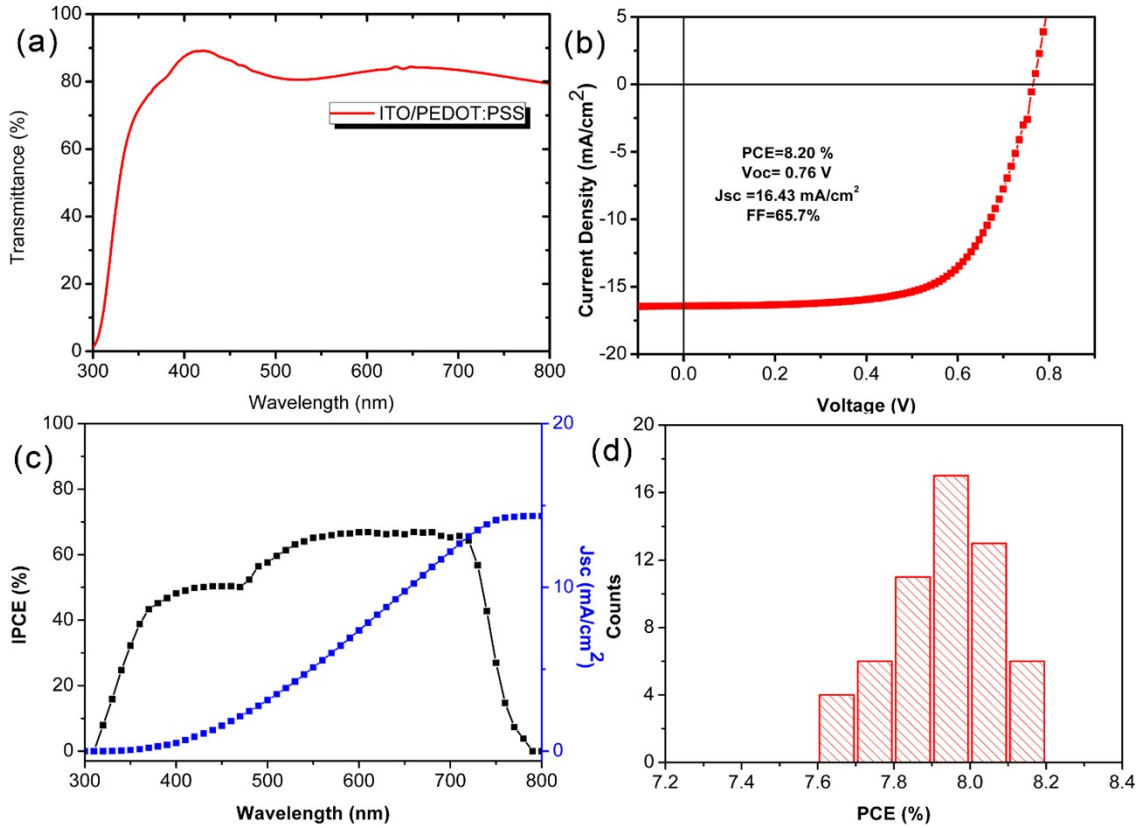


**Figure S7**. (a) Transmittance of ITO/PEDOT:PSS, (b) $J-V$ curves, (c) IPCE spectra and (d) The histograms of PCEs with PEDOT:PSS as the HTL.

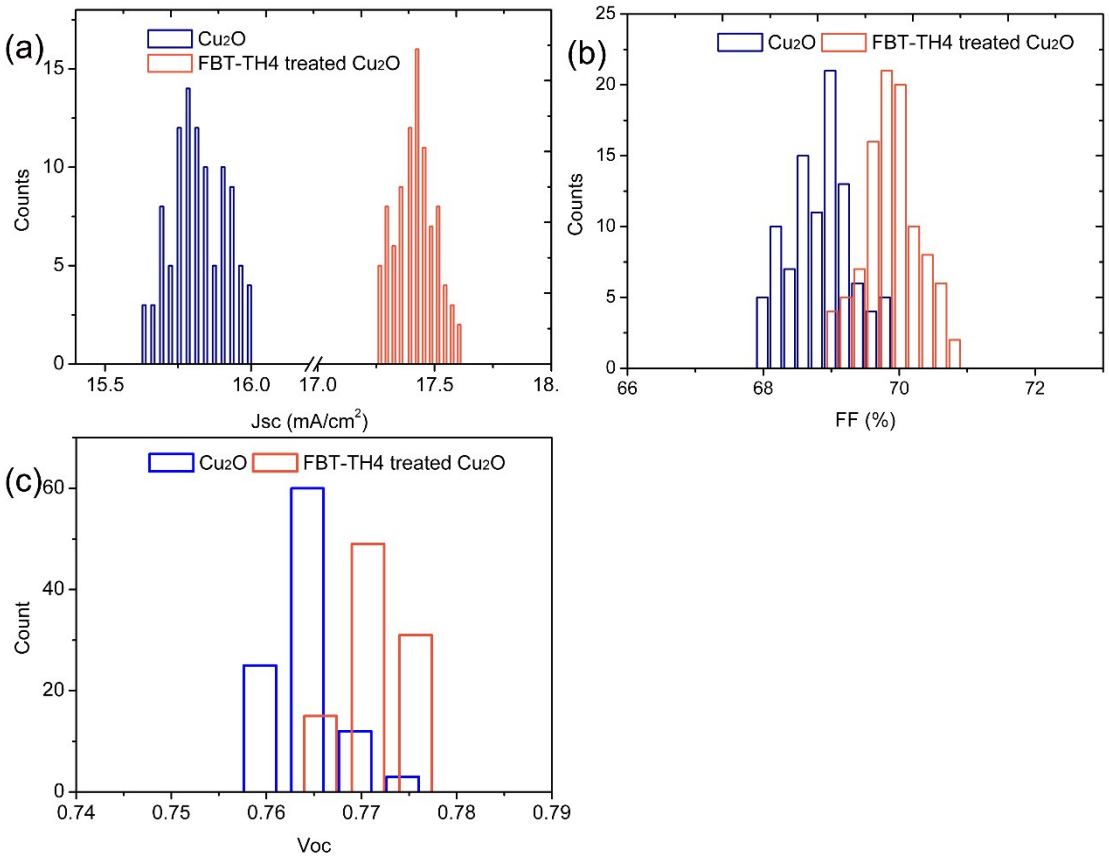


**Figure S8.** Histogram of (**a**) *J*sc, (**b**) FF and (**c**) *V*oc counts of 100 individual devices with untreated $Cu_2O$ and treated $Cu_2O$/FBT-TH4 HTMs, respectively.

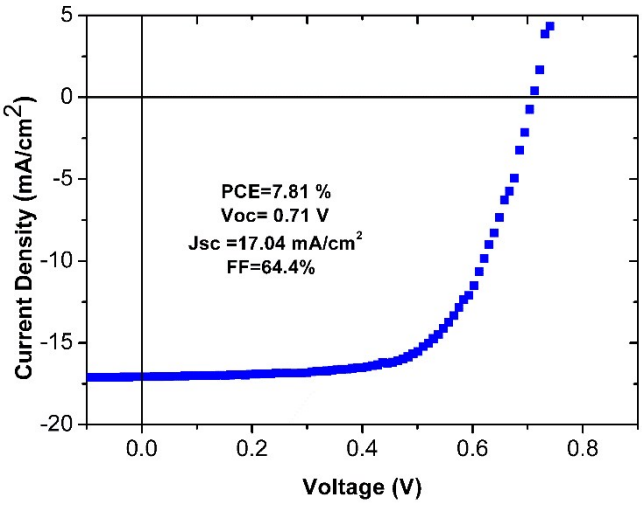


**Figure S9.** Typical J-V plots of planar solar cells with an architecture of ITO/FBT-TH4/PffBT4T-2OD:$PC_{71}BM$/PDINO/Al.

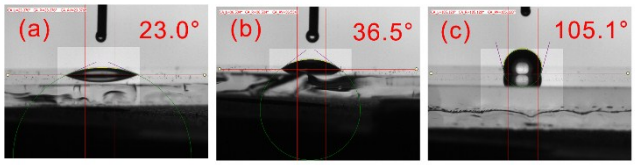


**Figure S10.** Contact angles of water droplets on (a) ITO/PEDOT:PSS, (b) ITO/$Cu_2O$ and (c) ITO/$Cu_2O$/FBT-TH4 surfaces.

**Table S4**. Stability of PffBT4T-2OD:$PC_{71}BM$ solar cells with the untreated and FBT-TH4 treated $Cu_2O$ layer as the HTM, respectively.

| *HTMs* | *Storing time* [Day] | *Voc* [V] | *Jsc* [mA $cm^{-2}$] | *FF* [%] | *PCE* [%] |
|---|---|---|---|---|---|
| Untreated $Cu_2O$ | 0 | 0.760 | 16.00 | 69.8 | 8.48 |
| | 1 | 0.729 | 15.68 | 64.9 | 7.42 |
| | 2 | 0.76 | 14.72 | 54.5 | 6.09 |
| | 3 | 0.745 | 14.4 | 52.3 | 5.61 |
| | 6 | 0.769 | 13.76 | 43.3 | 4.58 |
| | 8 | 0.769 | 13.36 | 41.2 | 4.23 |
| | 10 | 0.760 | 13.28 | 40.4 | 4.08 |
| | 12 | 0.752 | 13.12 | 36.3 | 3.58 |
| | 16 | 0.748 | 12.8 | 36.9 | 3.53 |
| | 20 | 0.737 | 12.48 | 36.3 | 3.34 |
| | 24 | 0.749 | 11.84 | 35.6 | 3.16 |
| | 32 | 0.729 | 11.04 | 34.9 | 2.81 |
| | 0 | 0.770 | 17.49 | 70.7 | 9.52 |
| | 1 | 0.762 | 17.15 | 68.6 | 8.99 |
| | 2 | 0.785 | 16.80 | 67.9 | 8.96 |
| | 3 | 0.778 | 16.27 | 67.2 | 8.50 |
| | 6 | 0.775 | 16.10 | 67.8 | 8.45 |

| | | | | | |
|---|---|---|---|---|---|
| FBT-TH4 treated | 8 | 0.779 | 15.83 | 67.5 | 8.33 |
| $Cu_2O$ | 10 | 0.783 | 15.75 | 66.4 | 8.19 |
| | 12 | 0.779 | 15.58 | 65.7 | 7.98 |
| | 16 | 0.770 | 15.40 | 65.7 | 7.79 |
| | 20 | 0.779 | 15.05 | 65.4 | 7.67 |
| | 24 | 0.770 | 14.53 | 65.7 | 7.35 |
| | 32 | 0.762 | 14.17 | 65.0 | 7.02 |